PII: S0955-2219(97)00130-1

0955-2219/98/$—see front matter

Characterization of SnO_2-Varistors with Different Additives

M. S. Castro* and C. M. Aldao

Institute of Materials Science and Technology (INTEMA), Universidad Nacional de Mar del Plata—CONICET, Juan B. Justo 4302, 7600 Mar del Plata, Argentina

(Received 14 February 1997; accepted 3 July 1997)

Abstract

Some aspects of the effects of additives on the sintering process and their influence on the microstructure and electrical properties of SnO_2 varistors are still not well understood. Aiming at a better interpretation of the involved phenomena, the effects on microstructures and electrical properties of adding Co_3O_4, CuO, MnO_2, Bi_2O_3 and Sb_2O_3 to SnO_2 have been studied. We found that Co_3O_4 and MnO_2 enhance the densification of these ceramics by increasing the number of oxygen vacancies and, as a consequence, the sintering rate increases. Sb_2O_3, on the other hand, reduces the oxygen vacancy concentration and then the sintering rate is decreased. CuO and Bi_2O_3 form a liquid phase during the sintering process enhancing the sintering rate. We found that electrical properties are improved by the addition of all the studied dopants, due to the modifications in the microstructure and in the defect concentration.

1 Introduction

Varistors are semiconductor devices possessing highly nonlinear current–voltage characteristics. Their electrical behavior is similar to that of two back-to-back Zener diodes, but with much greater current and energy capabilities. It is well known that conduction in the prebreakdown region directly reflects the existence of Schottky barriers resulting from the presence of intergranular states at the grain boundaries.[1] ZnO-based ceramics are successfully utilized in manufacturing varistors which are employed as surge arrestors in electrical transmission systems.[2,3] Recently, other varistor systems have been described in the literature. Among them, TiO_2 doped with BaO and Nb_2O_5 has been used for low-voltage varistors and SnO_2-based varistors in high voltage applications and as gas sensors and resistors.[4–8]

Tin oxide is an *n*-type semiconductor similar to ZnO and TiO_2 but it does not densify when sintered without additives.[9,10] Due to this particular property, SnO_2 has been used as gas sensors.[11] On the other hand, dense SnO_2-based ceramic materials are now candidates for many industrial applications. For this reason, several dopants (such as MnO_2, CuO, ZnO) have been proposed as sintering aids. Conversely, Duvigneaud *et al.*[12] have studied the effects of adding Sb_2O_3 to the SnO_2–CuO system and reported a decrease in the sinterability.

It is clear, then, that the sintering behavior of the SnO_2-based varistor can be strongly modified by the addition of several oxides. In this context, we present in this work a systematic study of the effects on the microstructure and electrical properties of adding Co_3O_4, CuO, MnO_2, Bi_2O_3 and Sb_2O_3 to the SnO_2-based ceramics. Experiments show desirable trends regarding density, shrinkage, and electrical properties after the addition of Co_3O_4, MnO_2 and CuO.

2 Experimental Procedure

Varistors were prepared from samples containing selected metal oxides (see Table 1). Oxides were ground and pressed into disks of 1 cm in diameter and 0·1 cm thick. They were sintered at 1100°C during 3 h and then cooled down at 10°C min^{-1} up to 700°C and then in steps of 50°C every 20 min from 700 to 200°C. Electrodes were silver painted.

*To whom correspondence should be addressed. Fax: +54-23-810046.

Table 1. Sample composition

Sample	SnO_2 *(%w/w)*	Co_3O_4 *(%w/w)*	MnO_2 *(%w/w)*	CuO *(%w/w)*	Sb_2O_3 *(%w/w)*	Bi_2O_3 *(%w/w)*
S1	100	—	—	—	—	—
S2	99·5	0·5	—	—	—	—
S3	99·5	—	0·5	—	—	—
S4	99·5	—	—	0·5	—	–
S5	99·4	0·5	—	—	0·1	—
S6	99·3	0·5	—	—	0·2	—
S7	99·1	0·5	—	—	0·4	—
S8	93·5	0·5	—	—	—	6
S9	93·5	—	0·5	—	—	6
S10	93·5	—	—	0·5	—	6
S11	94·0	—	—	—	—	6
S12	99·9	—	—	—	0·1	—

Currents were measured with a Keithley 614 electrometer. The power supply was a Phitronics (0–60 V, 0–2 A). Currents were very stable after a few seconds, and thus a 15 s setting time before each data acquisition was adopted. Dielectric constant and dissipation factor were measured with a Hewlett Packard 4284A LCR meter in the range 100 Hz–1 MHz. Samples were characterized by means of X-ray diffraction (XRD) (Philips, CuK_α radiation), Fourier transformed infrared spectroscopy (FTIR) (Bruker IFS 25), UV-visible diffuse reflectance spectroscopy (UV-Vis DRS) (Shimadzu 210A), electron paramagnetic resonance spectroscopy (EPR) (Bruker ER-200D, Band X), and fractured samples with scanning electron microscopy (SEM) (Philips 505). Density measurements were carried out using the Arquimedes method.

3 Results and Discussion

It has been established that tin oxide does not densify during sintering due to the high vapor pressure of this oxide at high temperatures.[7] This is described by

$$SnO_2(s) \leftrightarrow SnO(g) + 0{\cdot}5\ O_2 \qquad (1)$$

For this reason, the evaporation-condensation mechanism controls the sintering process. However, when SnO_2 is doped with other additives (as Co_3O_4, CuO, MnO_2, ZnO) the densification can be improved at 1100°C. Since the XRD analyses did not show other phases in the samples, the increase in the densification can be explained as follows for the cobalt oxide:

$$Co_3O_4 \rightarrow CoO + Co_2O_3 \qquad (2)$$

$$CoO \xrightarrow{SnO_2} Co''_{Sn} + V_o^{\bullet\bullet} + O_o \qquad (3)$$

$$Co_2O_3 \xrightarrow{SnO_2} 2Co_{Sn} + V_o^{\bullet\bullet} + 3O_o \qquad (4)$$

The manganese oxide have two reduction processes between room temperature and sintering temperature:

$$2\ MnO_2 \rightarrow Mn_2O_3 + 0{\cdot}5\ O_2 \qquad (5)$$

$$3\ Mn_2O_3 \rightarrow 2\ Mn_3O_4 + 0{\cdot}5\ O_2 \qquad (6)$$

in the lattice,

$$Mn_2O_3 \xrightarrow{SnO_2} 2Mn'_{Sn} + V_o^{\bullet\bullet} + 3\ O_o \qquad (7)$$

$$MnO \xrightarrow{SnO_2} Mn''_{Sn} + V_o^{\bullet\bullet} + O_o \qquad (8)$$

UV-Vis DRS analyses show that cobalt and manganese stabilize as Co^{+2} and Mn^{+2} as the result of incorporating Co_3O_4 and MnO_2 in SnO_2. These ions are compensated by oxygen vacancies in the lattice according to eqns (3)–(8).

N. Dolet and co-workers have studied the sintering mechanism of SnO_2–CuO mixtures and have determined that, when the sintering temperatures are equal to or higher than 940°C, the increase in the densification of SnO_2 by the addition of CuO is due to the existence of a liquid phase in the Sn–Cu–O_2 system.[9] Other researchers have determined by XRD that copper ions do not enter into the crystal structure of SnO_2.[11]

An increase in the density with the addition of Co_3O_4, MnO_2 or CuO to the SnO_2 is observed. However, the addition of Sb_2O_3 to the SnO_2–Co_3O_4 system produces a decrease of the density (see Table 2). To explain this behavior it is necessary to point out that Sb_2O_5 is the stable form up to 970°C, but Sb_2O_3 is more stable at higher temperatures. The Sb^{+5}/Sb^{+3} ratio will depend both on the temperature and on the concentration at ambient oxygen. In addition, the relatively high ionic radius of Sb^{+3} practically

Table 2. Density of SnO_2-based samples after sintering during 3 h at 1100°C

Sample	*Density (g cm^{-3})*
S1	1·97
S2	5·73
S3	4·98
S4	3·95
S5	4·58
S7	4·23
S8	5·62
S9	5·22
S10	5·43
S11	3·42

excludes the participation of these ions in a solid solution. However, in the surface layers exposed to the atmosphere, due to the incomplete coordination, fluctuations in the Sb^{+5}/Sb^{+3} ratio are possible and the conductivity may vary in an unusual manner due to the process.[13]

$$Sb^{+5} + 2e^{-} \leftrightarrow Sb^{+3} \tag{9}$$

The solid solution formation produces free electrons as follows:

$$Sb_2O_5 + V_o^x \xrightarrow{SnO_2} 2\,Sb^{\bullet}_{Sn} + 2e' + 5\,O_o \tag{10}$$

where the oxygen vacancy is not ionized to justify the generation of free electrons. According to this equation, the addition of antimony oxide reduces the oxygen vacancy concentration and then the grain growth is retarded.

Figure 1 shows the microstructure for samples having different additives. Sample S1 (SnO_2) shows little densification with a fine grains microstructure ($< 1\,\mu m$). The incorporation of additives which produce an increase in oxygen vacancy concentration, samples S2 and S3, enhances the mass transport resulting in an appreciable increase in densification and grain size. On the other hand, when 0·4% Sb_2O_3 (S7) is added to SnO_2–Co_3O_4, the densification and the grain size decrease. This effect is due to the decrease in the oxygen vacancy concentration produced by the Sb_2O_5 [see eqn (10)]. Interestingly, samples with a lower amount of Sb_2O_3 ($< 0{\cdot}2\%$) do not present a noticeable decrease in the grain size. The addition of Bi_2O_3 to SnO_2 (S11) produces an increase in the grain growth because Bi_2O_3 forms a liquid phase which enhances the grain rearrangement and the mass transfer. However, the incorporation of the other additives (Co_3O_4, MnO_2, or CuO) to the SnO_2–Bi_2O_3 system,

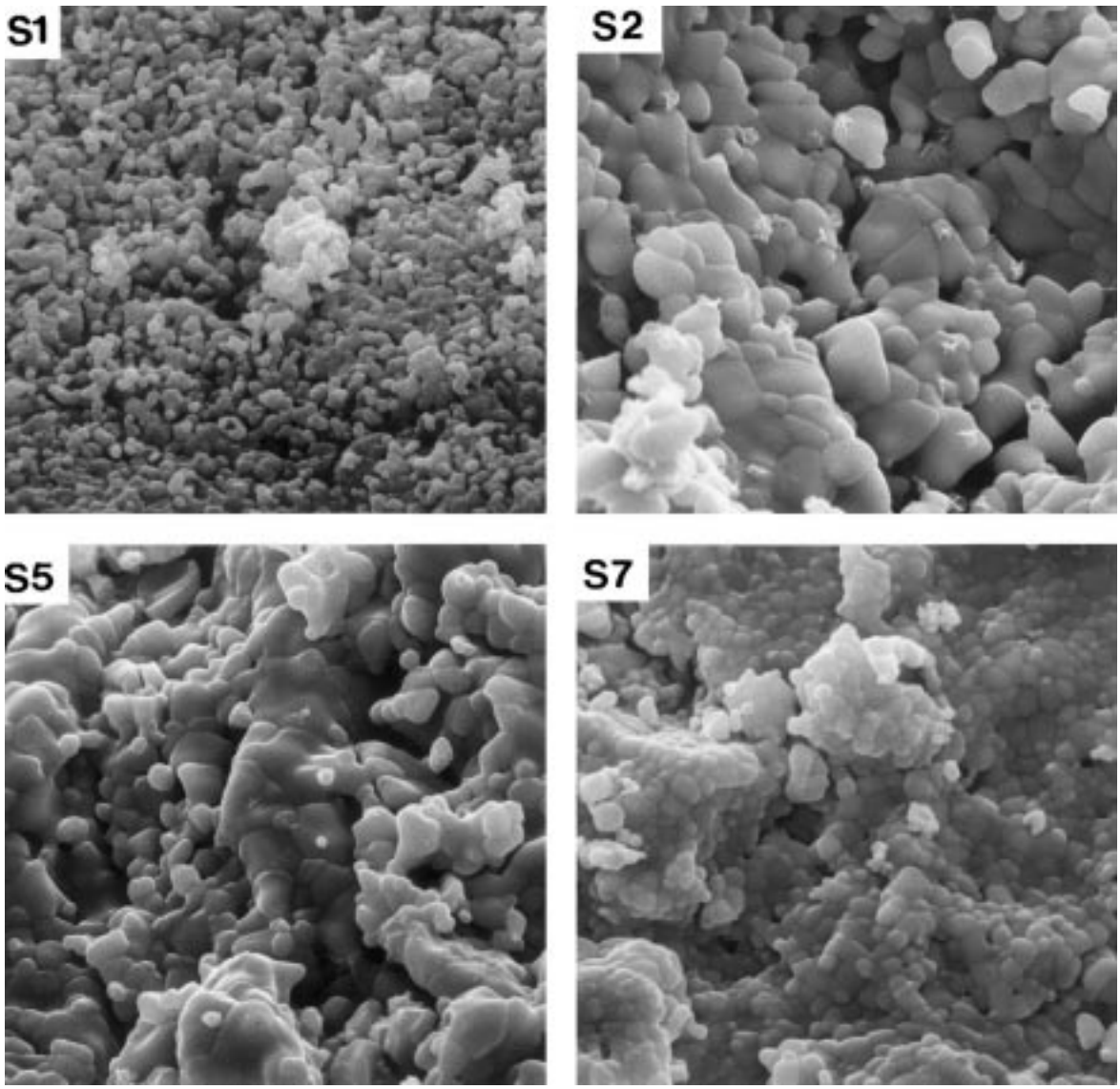

Fig. 1. Microstructure of the samples S1, S2, S5, S7, S8, S11 and S12. Samples S1 and S12: bar 1 μm; samples S2, S5, S7, S8 and S11: bar 10 μm.

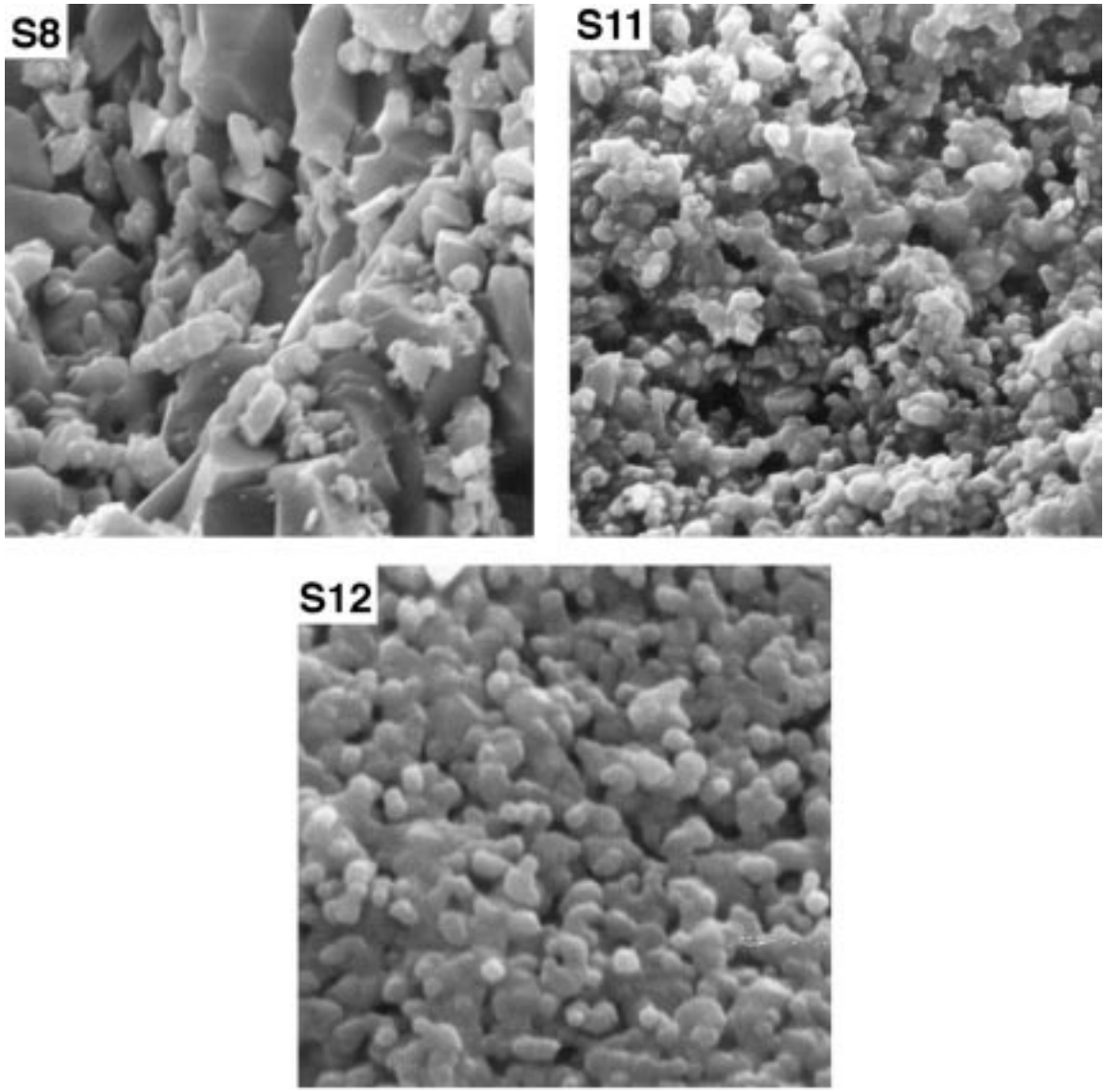

Fig. 1. *cont.*

produces an increase in the oxygen vacancy concentration, enhance the mass transport, and results in an appreciable increase in the densification and grain size. These samples present small grains (about 1–5 μm) and large grains with sizes greater than 10–20 μm (Fig. 1, sample S8). It is interesting to note that in sample S2 this abnormal grain growth does not appear. The behavior of the SnO_2–Bi_2O_3–Co_3O_4 is the consequence of two mechanisms: the presence of a liquid phase and the solid solution in the lattice of SnO_2 during the sintering process.

Table 3. Relative area of the EPR peaks corresponding to oxygen vacancy

Sample	W^2I
S1	0·17
S2	0·77
S5	4·2
S7	1·98
S12	0·12

In order to analyze the presence of oxygen vacancies we carried out EPR spectroscopy in the region of the $V_o^{\bullet}$ peak[14] to check for the process

$$V_o^{\bullet\bullet} \rightarrow V_o^{\bullet} + h^{\bullet} \qquad (11)$$

To roughly evaluate the species concentration, we calculated the relative area of the spectra according to the expression W^2I, where W is the peak-to-peak width and I is the height of the recorded first derivative of the adsorption EPR signal. Results show that the addition of cobalt or manganese oxides increases the $V_o^{\bullet}$ peak (see Table 3) consistent with the solid state mechanism proposed. On the other hand, the addition of 0·1% of Sb_2O_3 to samples with 0·5% of Co_3O_4 (S5) produces an increase in the $V_o^{\bullet}$ peak, but the addition of 0·4% of Sb_2O_3 (S7) reduces this peak. From the resulting microstructure (Fig. 1) we can see that the addition of 0·1% of Sb_2O_3 does not produce an increase in the

grain growth as expected due to the oxygen concentration. This behavior indicates that another mechanism could be present. A possible explanation for this effect follows. For an addition of antimony oxide of 0·1% the ratio Sb^{+5}/Sb^{+3} is small, and then some Sb_2O_3 particles could restrict the normal grain growth and Sb^{+3} in the surface of the grains could remove a positive charge from the oxygen vacancies. This behavior could explain the increase of the oxygen vacancies peak (Table 3) without an increase of the density (Table 2). Samples with more than 0·2% of Sb_2O_3 and Co_3O_4 show a decrease in the oxygen vacancy concentration. On the other hand, in samples with SnO_2 and 0·1% of Sb_2O_3 but without Co_3O_4 (S12) we can see an oxygen vacancy decrease which produces a decrease in the grain growth, according to the solid reaction mechanism proposed. The difference between S5 and S12 behaviors is due to the presence of Co_3O_4 that, for low concentration of Sb_2O_3, modifies the ratio Sb^{+5}/Sb^{+3} producing an increase in the oxygen vacancy concentration.

Studies with FTIR of samples with cobalt, manganese, or copper oxides (Fig. 2) showed a shift in the bands at 505 cm^{-1} which is related to the vibration of O^{-2} involving Sn-O stretching.[15] However, the addition of Sb_2O_3 showed a shift in the bands at 705 cm^{-1} which is related to the displacement of Sn^{+4} relative to O^{-2} along the c-axis. These results indicate that these additives interact with the lattice modifying the vibrational frequency of tin–oxygen bonds.

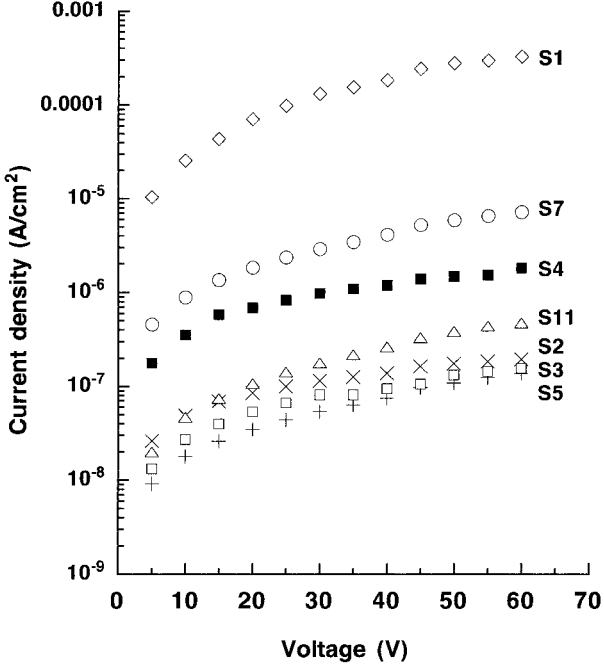

Fig. 3. Current density versus voltage curves of SnO_2-based varistors (S1, S2, S3, S4, S5, S7 and S11)

SnO_2-based ceramics present a varistor behavior with three zones in the current-voltage curves: the pre-breakdown, breakdown, and up-turn.[2] In this work, we analyze the pre-breakdown region because its sensitivity to changes in the sample composition. It is important to note that at the prebreakdown region it is desirable that varistors present low conductivity. In Fig. 3, measured currents densities for a number of specimens are plot-

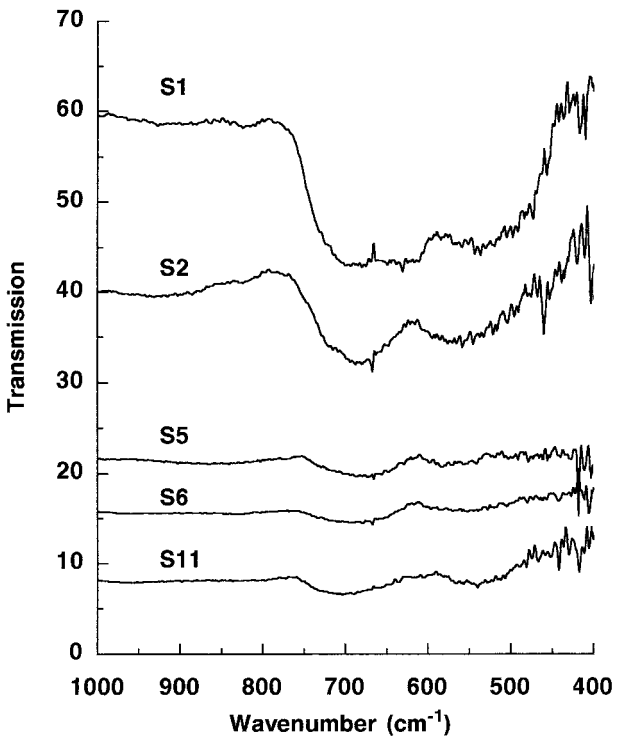

Fig. 2. FTIR spectra of the samples S1, S2, S5, S6 and S11.

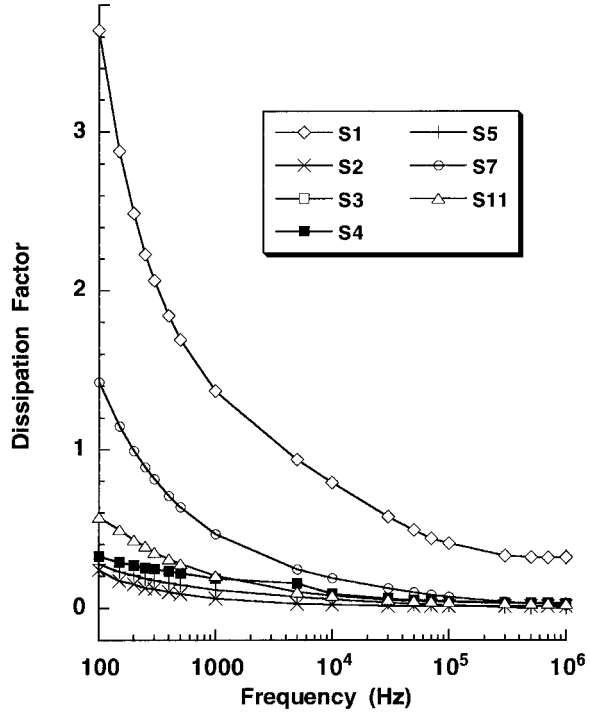

Fig. 4. Dissipation factor versus frequency curves of samples S1, S2, S3, S4, S5, S7 and S11.

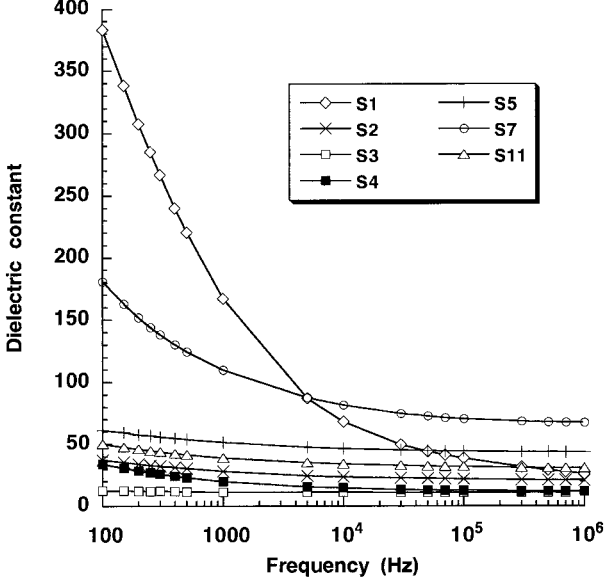

Fig. 5. Dielectric constant versus frequency curves of samples S1, S2, S3, S4, S5, S7 and S11.

ted as a function of the applied voltage in the range 5–60 V. From this figure we can see that the effective conductivity of samples with additives is much lower than the conductivity of sample S1. From this point of view, the electrical properties of the SnO_2 varistors are improved by adding Co_3O_4, MnO_2, or CuO. On the other hand, the addition of Sb_2O_3 over a 0·2% produces an increase in the electrical conductivity. This behavior is related to the process detailed in eqns (9) and (10) in which free electrons are produced. On the other hand, when the addition of Sb_2O_3 is lower than 0·2%, this oxide produces a decrease in the conductivity which is related to an increase in the hole concentration that reduces the number of free electrons.

Figure 4 shows the dissipation factor versus frequency curves for samples S1, S2, S3, S4, S5, S7, and S11. From these curves, it is possible to see that sample S1 presents a higher dissipation factor than the other samples in all the range of frequencies. The dissipation factors present the same order as the conductivity measurements (S1 > S7 > S11 > S4 > S3 > S2 > S5). The dissipation factor at low frequencies is due to the dc-conductivity and the space charge relaxation, while at high frequencies the ion jump and dipole relaxation losses effects are important. Sample S1 presents the highest loss factor at any frequency indicating that dc-conductivity and relaxation are important. From the dielectric constant versus frequency curves (Fig. 5), it is possible to conclude that samples present a Debye-type behavior modified by the presence of more than one polarization process accounting for the differences observed in our samples.[12] Due to the small grain size, samples S1 and S7 present a high dielectric constant at low frequencies reflecting the effect of many grain boundaries.[16,17] At higher frequencies, the dielectric constant of sample S1 decreases with respect to the other samples, this behavior could be a consequence of its high porosity. On the other hand, sample S7 has a higher dielectric constant than the samples S11, S2, S3, S4, S5, which can be related to the presence of Sb^{+5} in the lattice implying an increase in the dopant concentration.

4 Conclusions

From the experimental results we can conclude the following.

1. Co_3O_4 and MnO_2 enhance the sintering rate of these ceramics by increasing the number of oxygen vacancies and, as a consequence, the densification is larger. The addition of a higher concentration than 0·2% of Sb_2O_3, on the other hand, reduces the oxygen vacancy concentration and then the sintering rate decreases. The addition of 0·1% Sb_2O_3 does not affect the sintering due to the low antimony concentration which is not enough to establish an adequate Sb^{+5}/Sb^{+3} ratio. CuO and Bi_2O_3 form a liquid phase during the sintering process which increases the mass transport and then the sintering rate increases.
2. Electrical properties are improved by the addition of the several dopants. The addition of MnO_2, Co_3O_4, CuO or $Co_3O_4 + 0{\cdot}1\%\ Sb_2O_3$, produces varistors with a low dissipation in the pre-breakdown region. This behavior is related to the increase of electrons in the sample with $0{\cdot}5\%Co_3O_4 + 0{\cdot}4\%Sb_2O_3$ and with the number of grain boundaries which control electrical conduction. The dissipation factor is reduced by the addition of the several additives. Changes in the dielectric constant with the frequency are related with the space charge relaxation, dipole polarization, and porosity.

References

1. Castro, M. S. and Aldao, C. M., Prebreakdown conduction in zinc oxide varistors: thermionic or tunnel currents and one-step or two-step conduction processes. *Appl. Phys. Lett*., 1993, **63**, 1077–1079.
2. Levinson, L. M. and Philipp, H. R., Zinc-oxide varistors—a review. *Am. Ceram. Soc. Bull*., 1986, **65**, 639–646.
3. Gupta, T. K., Application of zinc oxide varistors. *J. Am. Ceram. Soc*., 1990, **73**, 1817–1840.
4. Ling, H. C., Yan, M. F. and Rhodes, W. W., Monolithic device with dual capacitor and varistor functions. *J. Am. Ceram. Soc*., 1989, **72**, 1272–1276.

5. Kutty, T. R. N. and Ravi, V., Varistors based on n-$BaTiO_3$ ceramics. *Mat. Sci. and Eng.*, 1993, **B20**, 271–279.
6. Yang, S. L. and Wu, J. M., Novel niobium-doped titania varistors with added barium and bismuth. *J. Am. Ceram. Soc.*, 1993, **76**, 145–152.
7. Pianaro, A., Bueno, P. R., Longo, E. and Varela, J. A., A new SnO_2-based varistor system. *J. Mat. Sci. Lett.*, 1995, **14**, 692–964.
8. Egashira, M., Shimizu, Y., Takao, Y. and Fukuyama, Y., Hydrogen-sensitive breakdown voltage in the I–V characteristics of tin dioxide-based semiconductors. *Sensors and Actuators*, 1996, **B33**, 89–95.
9. Dolet, N., Heintz, J. M., Rabardel, L., Onillon, M. and Bonnet, J.P., Sintering mechanisms of $0{\cdot}99SnO_2$–$0{\cdot}01CuO$ mixtures. *J. Mat. Sci.*, 1995, **30**, 365–368.
10. Muccilo, R., Cerri, J. A., Leite, E. R. and Varela, J. A., Impedance spectroscopy of SnO_2:CO during sintering. *Mater. Lett.*, 1997, **30**, 125–130.
11. Sahar, M. R. and Hasbullah, M., Properties of SnO_2-based ceramics. *J. Mat. Sci.*, 1995, **30**, 5304–5306.
12. Duvigneaud, P. H. and Reinhard, D., Activated sintering of tin oxide. In *Science of Ceramics* **1**2, ed. Ceramurgia s.r.l, Faenza, Italy, 1980 pp. 287–292.
13. Ovenston, A., Sprînceanâ, D., Walls, J. R. and Câldâraru, M., Effects of frequency on the electrical characteristics of tin-antimony-oxide mixtures. *J. Mat. Sci.*, 1994, **29**, 4946–4952.
14. DiNola, P., Morazzoni, F., Scotti, R. and Narducci, D., Paramagnetic point defect in SnO_2 and their reactivity with the surrounding gases. Part 1. *J. Chem. Soc. Faraday Trans.*, 1993, **89**, 3711–3713.
15. Farmer, V. C., The anhydrous oxide minerals. In *The Infrared Spectra of Minerals*, ed. V. C. Farmer. Mineralogical Society, London, 1974, pp. 183–197.
16. Kingery, W. D., Bowen, H. K. and Utilman, D. R., *Introduction to ceramics*. John Wiley and Sons, New York, 1976, pp. 913–974.
17. Buchanan, R. C., Properties of ceramics insulators. In *Ceramic Materials for Electronics*. ed. R. C. Buchanan. Marcel Dekker, New York, 1986, pp. 1–77.